The oxidation of L-ascorbic acid by trisoxalatoferrate(III) in weakly acidic aqueous solution revisited. Evidence for parallel inner-sphere and outer-sphere electron-transfer reaction paths

B. Bänsch, R. van Eldik*
Institute for Inorganic Chemistry, University of Witten/Herdecke, Stockumer Strasse 10, 5810 Witten (Germany)
and P. Martinez
Departamento de Quimica Fisica Aplicada, Universidad Autònoma, Madrid 28049 (Spain)

(Received January 24, 1992; revised May 25, 1992)

Abstract

The oxidation of L-ascorbic acid by trisoxalatoferrate(III) was reinvestigated as a function of pH, ascorbic acid and oxalate concentration, in terms of a multistep process that involves the formation of an intermediate ascorbate–oxalate complex. The kinetic data indicated rapid formation of the intermediate complex, followed by a slower electron-transfer process between the redox partners that occurs in two parallel reaction paths involving an inner-sphere and outer-sphere process. A direct comparison of the electron-transfer rate constants for these processes was possible following a calculation of the outer-sphere precursor formation constant. The self-exchange rate constant for the $Fe(C_2O_4)_3^{3-/4-}$ system was estimated to be 2.1×10^4 M^{-1} s^{-1} at 25 °C and is discussed in reference to similar data for related systems.

Introduction

The strong reducing properties of L-ascorbic acid (Vitamin C) in aqueous solution is of fundamental interest in biochemical and related processes, and has resulted in a series of studies on the oxidation reactions of L-ascorbic acid by transition metal complexes. Many of these reactions proceed according to an outer-sphere electron-transfer process due to either the absence or non-lability of available coordination sites on the metal center, viz. $Fe(CN)_6^{3-}$, $Fe(phen)_3^{3+}$, $Co(bpy)_3^{3+}$, $Co(phen)_3^{3+}$, $Co(C_2O_4)_3^{3-}$ and $Co(H_2O)_6^{3+}$ [1–5]. In some cases where the metal complex has labile coordination sites, viz. $Fe(H_2O)_5OH^{2+}$ [6], $Mn(CyDTA)H_2O^-$ and $Mn(bpy)_2(H_2O)OH^{2+}$ [7], kinetic evidence for the operation of an inner-sphere electron-transfer process was presented. In general it is not possible to observe the formation of an inner-sphere intermediate due to the rapid subsequent electron-transfer step, although this has been done for some cases, viz. $Ru(Cl)_2(H_2O)_4^+$, $Ru(IMDA)^+$, $Ru(EDTA)^-$ [8] and aquated Fe(III) [9].

The formation of intermediate ascorbate complexes of Fe(III) has been observed by different groups. Xu and Jordan [9] observed the formation and decay of such an intermediate at 560 nm under conditions where an excess of Fe(III) was employed. In more acidic medium, i.e. where ascorbic acid is not deprotonated and Fe(III) mainly exists as $Fe(H_2O)_6^{3+}$, the formation of the intermediate could not be observed in the presence of an excess ascorbic acid [6]. The formation of an intermediate species was also observed for the oxidation of L-ascorbic acid by $Fe(C_2O_4)_3^{3-}$, which exhibits a characteristic absorption at 490 nm [10]. The authors concluded that the electron-transfer reaction only involves the intramolecular inner-sphere process. A reinvestigation of this system, using more sophisticated software that enabled an improved and more complete analysis of complex kinetic traces, revealed that the overall process is more complicated and also involves a parallel outer-sphere reaction route. The main results of this reinvestigation are reported here.

Experimental

Materials

$K_3[Fe(C_2O_4)_3]$ was used as obtained from Alfa Products. L-Ascorbic acid and all other chemicals were of analytical reagent grade (Merck). Stock solutions were

*Author to whom correspondence should be addressed.

0020-1693/92/$5.00

prepared with Millipore water immediately before use. An acetate buffer was employed to control the pH. In the stopped-flow kinetic measurements, $NaNO_3$ was used to adjust the ionic strength to 1.0 M. Air and argon saturated solutions resulted in the same kinetic behaviour. In the electrochemical measurements, $LiClO_4$ was used to adjust the ionic strength to 1.0 M, and test solutions were flushed with N_2 for 20 min prior to the start of the reaction.

Measurements

pH measurements were performed with a Metrohm 632 instrument equipped with a Sigma glass electrode. UV–Vis spectra were recorded on a Cary 1.3 spectrophotometer. Rapid scan spectra were recorded on a Durrum D 110 stopped-flow unit attached to an OSMA detector (Spectroscopic Instruments GmbH, Gielsching, Germany). Kinetic measurements were performed on a thermostated (±0.1 °C) Durrum D 110 stopped-flow instrument. The kinetic traces were recorded on an IBM compatible computer and analysed with the OLIS KINFIT set of programs [11]. In general the kinetic traces exhibited a series of subsequent reactions which could be resolved using an iteration procedure. The redox process was followed at 480 nm where the formation and decomposition of the intermediate species was observed. All kinetic experiments were performed under pseudo-first-order conditions, i.e. an excess of ascorbic acid and oxalate (see 'Results and discussion').

The reduction of Fe(III) was followed by cyclovoltammetry (CV). The measurements were performed in an H-shaped cell that was connected to a sample reservoir. Both parts of the instrument could be flushed with N_2. One of the reaction components was added rapidly to the other one in the cell via the sample reservoir. Solutions were flushed with N_2 during the measurements to ensure rapid transport at the working electrode. Gold foil was used as working and counter electrode, whereas a $HgSO_4$ electrode in a saturated solution was employed as reference system. The electrodes and glass equipment were cleaned in a KOH bath and thoroughly washed with Millipore water prior to use. A programmable function generator was used to create the triangular potential. This instrument was developed jointly by Fa. Hopf (Lüdenscheid) and the Electronic Workshop of the University of Witten/Herdecke. A potentiostat Type LB 75L, Fa. Wenking, was used in the measurements and the voltammograms were recorded on a Kipp & Zonen recorder.

Results and discussion

Preliminary measurements

The oxidation of L-ascorbic acid (AH_2) by Fe(III) complexes results in the formation of L-dehydroascorbic acid (A) according to the overall reaction (1) [10]. During the reaction of AH_2 with $Fe(C_2O_4)_3^{3-}$ a red

$$AH_2 + 2Fe(III) \longrightarrow A + 2H^+ + 2Fe(II) \quad (1)$$

intermediate is produced that undergoes a subsequent slow decomposition. The formation of this intermediate could be studied on the rapid-scan instrument (see Fig. 1(a)), whereas its decomposition was followed on a conventional spectrophotometer (Fig. 1(b)). These spectra clearly indicate that the intermediate species exhibits a maximum around 480 nm, which is in close agreement with our earlier finding [10]. A detailed study of the kinetic traces at this wavelength as a function of the different concentration variables indicated that the overall process exhibits not less than three consecutive reaction steps, namely the rapid formation of the intermediate, followed by a relatively fast and subsequently slow decomposition reaction. Furthermore, the analysis of these absorbance–time plots using various fitting

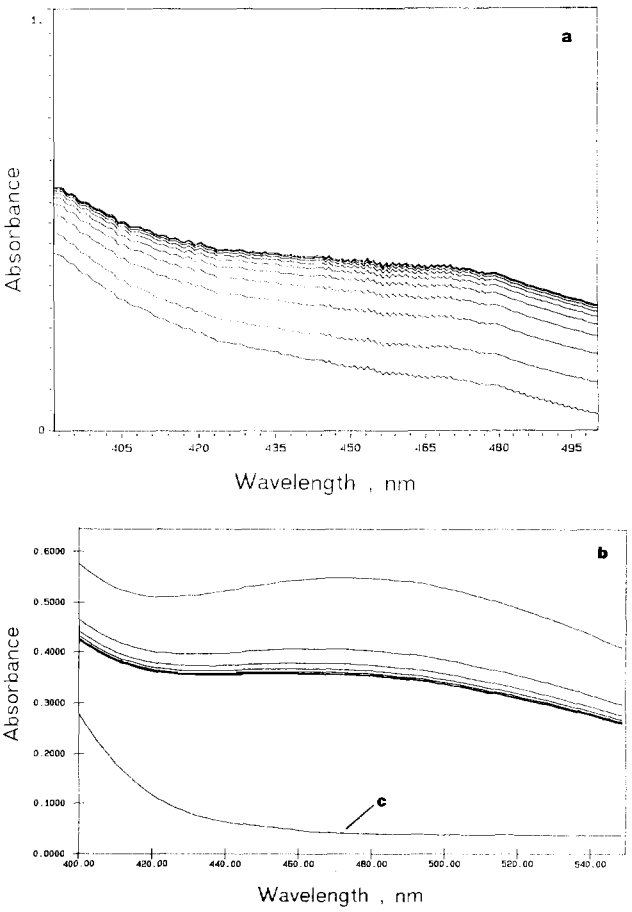

Fig. 1. Repetitive scan spectra recorded for the formation and decomposition of the intermediate produced in the reaction of L-ascorbic acid with $Fe(C_2O_4)_3^{3-}$. Experimental conditions: $[AH_2]_{tot} = 0.10$ M; $[oxalate]_{tot} = 1.0 \times 10^{-2}$ M; $[Fe(C_2O_4)_3^{3-}] = 2.0 \times 10^{-3}$ M; pH = 4.5 (acetate buffer); ionic strength = 1.0 M; temperature = 25 °C; $\Delta t = 32$ ms (a), 2 min (b); c = spectrum before mixing the reaction components.

routines [11], indicated that reasonable fits can only be obtained in the presence of added oxalate. This means that the $Fe(C_2O_4)_3^{3-}$ species exhibits some spontaneous aquation reaction that can be suppressed by the addition of oxalate under our selected experimental conditions. For this purpose at least a five-fold excess of oxalate was employed. In our earlier work [10], this complication was not detected since only the initial formation and final decay parts of the kinetic traces were analysed separately in terms of the formation and redox decomposition of the inner-sphere complex. A few typical kinetic traces recorded in the presence of added oxalate are reported in Fig. 2, from which it follows that the overall oxidation of L-ascorbic acid by $Fe(C_2O_4)_3^{3-}$ can be described by a series of three consecutive reaction steps. During the first step (Fig. 2(a)) the absorbance increases rapidly due to the formation of an intermediate species, which is followed by an absorbance decrease (Fig. 2(b) and (c)). The latter decrease consists of two consecutive reactions as demonstrated by the quality of the fit when the absorbance decrease it fitted with a single exponential (Fig. 2(b)) or two exponentials (Fig. 2(c)). These three reaction steps were studied in detail as a function of ascorbic acid concentration, oxalate concentration and pH. In the selected weakly acidic pH range (3.5–5.0), ascorbic acid is mainly present as the monodeprotonated ascorbate ion (AH^-), which is significantly more reactive than ascorbic acid itself [1–6, 10].

Formation of intermediate

The observed pseudo-first order rate constant for the formation of the intermediate surprisingly decreases with increasing ascorbic acid concentration and increasing pH, but increases with increasing oxalate concentration (see summary of data in Table 1). This behaviour is typical for a substitution process that involves two parallel reaction routes, which can be summarized by the reactions in (2)*. The formation of the inner-sphere $Fe(C_2O_4)_2AH^{2-}$ species proceeds

$$AH_2 \overset{K_a}{\rightleftharpoons} AH^- + H^+$$

$$Fe(C_2O_4)_3^{3-} + 2H_2O \underset{k_{-1}}{\overset{k_1}{\rightleftharpoons}} Fe(C_2O_4)_2(H_2O)_2^- + C_2O_4^{2-}$$

$$\begin{array}{lll} +AH^-,\ -C_2O_4^{2-} & & +AH^-,\ -2H_2O \\ k_{-3} \uparrow \quad \downarrow k_3 & & k_2 \uparrow \quad \downarrow k_{-2} \\ & Fe(C_2O_4)_2AH^{2-} & \end{array} \qquad (2)$$

*This reaction scheme was developed on the basis of similar concentration dependences recently observed for a substitution process involving parallel reaction paths [12].

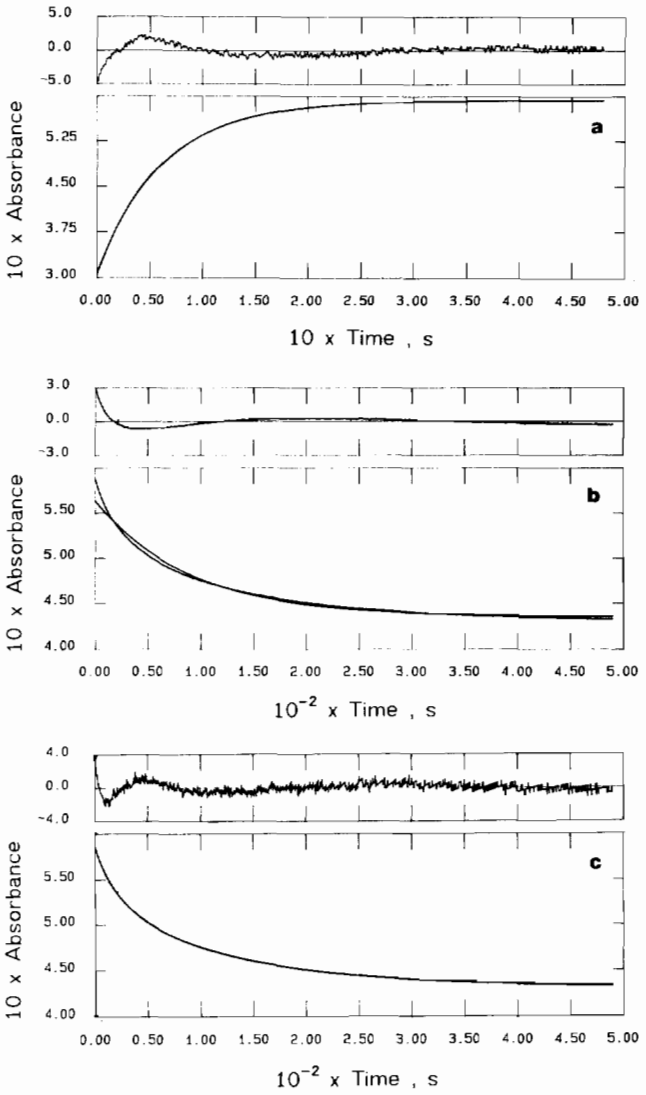

Fig. 2. Absorbance–time plots recorded for the formation and decomposition of the $Fe(C_2O_4)_3^{3-}$–ascorbic acid intermediate at 480 nm. Experimental conditions: $[AH_2]_{tot} = 0.30$ M; $[oxalate]_{tot} = 2.0 \times 10^{-2}$ M; $[Fe(C_2O_4)_3^{3-}] = 2.0 \times 10^{-3}$ M; pH = 4.5 (acetate buffer); ionic strength = 1.0 M; temperature = 25 °C; reaction time scale 1 s (a), 500 s (b), (c); for each kinetic trace the difference between the experimental and theoretically predicted fit is plotted in the diagram above the trace.

via the aquation of $Fe(C_2O_4)_3^{3-}$ followed by the reaction with AH^-, and via the direct attack of AH^- on $Fe(C_2O_4)_3^{3-}$. Since only a small fraction of the ascorbic acid is present in the protonated form (AH_2) under the selected conditions, and AH^- is significantly stronger nucleophile than AH_2 in substitution reactions of Fe(III) [9], reactions involving the AH_2 species are not included in eqn. (2). The pH dependence of the observed rate constant (Table 1) can be correlated with the increase in concentration of AH^- with increasing pH and protonation of $Fe(C_2O_4)_3^{3-}$ that will assist the labilization of coordinated oxalate at lower pH.

TABLE 1. k_{obs} for the formation of the intermediate as a function of pH, ascorbic acid and oxalate concentration[a]

$[oxalate]_{tot} \times 10^2$ (M)	k_{obs}[b] (s^{-1}) at $[H_2A]_{tot}$ (M)			
	0.10	0.15	0.20	0.25
1.00	12.7 ± 0.1	11.4 ± 0.05	10.4 ± 0.2	10.3 ± 0.06
1.25	14.7 ± 0.1	12.3 ± 0.05	12.0 ± 0.1	11.2 ± 0.05
1.50	16.7 ± 0.2	14.0 ± 0.1	13.2 ± 0.04	12.5 ± 0.08
1.75	18.7 ± 0.2	16.0 ± 0.1	14.6 ± 0.08	13.8 ± 0.1
2.00	21.6 ± 0.2	17.5 ± 0.1	16.0 ± 0.05	15.0 ± 0.05
	k_{obs}[b] (s^{-1})	pH		
1.00	26.0 ± 0.5	3.5		
	17.4 ± 0.1	4.0		
	15.0 ± 0.1	4.25		
	12.7 ± 0.1	4.5		
	12.0 ± 0.1	5.0		

[a]Experimental conditions: $[Fe(III)] = 2 \times 10^{-3}$ M; pH = 4.5 (acetate buffer) unless otherwise indicated; temperature 25.0 °C; ionic strength = 1.0 M. [b]Mean value of at least five kinetic runs.

A general rate law for the reaction scheme in eqn. (2) at a fixed pH is given by the expression (3) [12]. This rate law only fits the experimental observations in terms of the oxalate and ascorbate concentration dependences when $k_2[AH^-] \gg k_{-1}[C_2O_4^{2-}]$, such that eqn. (3) then simplifies to eqn. (4)*. This equation predicts that k_{obs} should increase with increasing

$$k_{obs} = \frac{k_1 k_2 [AH^-] + k_{-1} k_{-2} [C_2O_4^{2-}]}{k_{-1}[C_2O_4^{2-}] + k_2[AH^-]} + k_{-3}[C_2O_4^{2-}] + k_3[AH^-] \quad (3)$$

$$k_{obs} = k_1 + k_3[AH^-] + (k_{-1}k_{-2}/k_2[AH^-] + k_{-3})[C_2O_4^{2-}] \quad (4)$$

oxalate concentration, and can decrease with increasing $[AH^-]$ depending on the importance of the $k_3[AH^-]$ term. Plots of k_{obs} versus $[C_2O_4^{2-}]$ as a function of $[AH^-]$ are indeed linear (see Fig. 3): the intercept increases with increasing $[AH^-]$ and the slope decreases with increasing $[AH^-]$ as predicted by eqn. (4). The corresponding fit of the intercepts results in $k_1 = 3.0 \pm 0.3$ s^{-1} and $k_3 = 11 \pm 2$ M^{-1} s^{-1} at 25.0 °C. A fit of the slopes results in $k_{-1}k_{-2}/k_2 = k_{-1}/K_2 = 59 \pm 3$ M^{-1} s^{-1} and $k_{-3} = 220 \pm 19$ M^{-1} s^{-1}. With the literature value

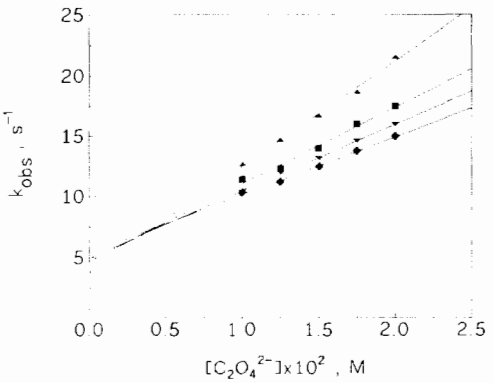

Fig. 3. Plots of k_{obs} vs. oxalate concentration for the formation of the intermediate (first step of the reaction). Experimental conditions: see Table 1; $[AH^-] = 0.091$ (▲), 0.136 (■), 0.182 (▼), 0.227 (◆) M.

of $K_1 = 1.41 \times 10^{-5}$ M^{-1} [13], k_{-1} ($= K_1/k_1$) was estimated to be 2.1×10^5 M^{-1} s^{-1} and $K_2 = (3.6 \pm 0.2) \times 10^3$ M^{-1}.

The above analysis of the kinetic data for the formation of the intermediate $Fe(C_2O_4)_2AH^{2-}$ species indicates that the oxalate concentration merely controls the equilibrium between $Fe(C_2O_4)_3^{3-}$ and $Fe(C_2O_4)_2(H_2O)_2^-$. This means that at high oxalate concentration substitution by AH^- will mainly proceed via the k_3 reaction step, whereas the k_2 path will become more important at lower oxalate concentrations, i.e. where a significant fraction of the Fe(III) complex is present as the bisoxalato complex. In order to fulfill the requirement that $k_2[AH^-] \gg k_{-1}[C_2O_4^{2-}]$, it can be shown by substituting typical concentrations employed in this study, that $k_2 \geqslant 10^4 \times k_3$, i.e. $k_2 \geqslant 1 \times 10^5$ M^{-1} s^{-1}, which results in $k_{-2} \geqslant 30$ s^{-1}, thus significantly larger than k_1. It follows that the aquation of $Fe(C_2O_4)_2AH^{2-}$ is significantly faster than the aquation

*When, alternatively, it is assumed that $k_2[AH^-] \ll k_{-1}[C_2O_4^{2-}]$, then eqn. (3) reduces to $k_{obs} = \{k_1k_2[AH^-] + k_{-1}k_{-2}[C_2O_4^{2-}]\}/k_{-1}[C_2O_4^{2-}] + k_{-3}[C_2O_4^{2-}] + k_3[AH^-]$ from which it follows that k_{obs} must increase with increasing $[AH^-]$, which is not the case. Furthermore, when $k_2[AH^-] \approx k_{-1}[C_2O_4^{2-}]$, then the experimental data must be described by eqn. (3), which predicts a non-linear dependence of k_{obs} on $[C_2O_4^{2-}]$. A corresponding fit of the data (see further 'Discussion') demonstrated that this is not the case. Thus the only limiting possibility is that $k_2[AH^-] \gg k_{-1}[C_2O_4^{2-}]$.

of $Fe(C_2O_4)_3^{3-}$. Finally, the k_3 reaction path will result in an increase in k_{obs} with increasing $[AH^-]$ at low oxalate concentration, i.e. at $[C_2O_4^{2-}]<5\times10^{-3}$ M according to the plots in Fig. 3.

Decomposition of intermediate

As mentioned above, the decomposition of the intermediate is observed in terms of a decrease in absorbance and exhibits two consecutive reaction steps. An important question to be answered is which reaction represents the reduction of Fe(III), i.e. oxidation of L-ascorbic acid. A few preliminary experiments indicated that the decomposition of the intermediate involves a redox process, in agreement with earlier results [10]. When $K_4Fe(CN)_6$ is added to the reaction solution containing $Fe(C_2O_4)_3^{3-}$ and AH^-, a white precipitate is produced, which indicates the formation of Fe(II). A qualitative analysis of Fe(II) was not possible with the usual methods employed since these were all affected by the presence of ascorbic acid/ascorbate. We therefore adopted an electrochemical method to identify the reaction step associated with the redox process.

The electron-transfer reaction was followed via the decrease in Fe(III) concentration using cyclovoltammetry (CV). Curve 1 in Fig. 4 represents the CV of a $Fe(C_2O_4)_3^{3-}$ solution, whereas curves 2–7 were recorded immediately after the addition of L-ascorbic acid. A clear decrease in the reduction current, i.e. the Fe(III) concentration, is observed on the addition of ascorbate (the sudden decrease observed for curves 2 and 3 is due to the dilution of the $Fe(C_2O_4)_3^{3-}$ solution). The increase in the oxidation current is caused by the oxidation of ascorbic acid during the redox process. The CVs indicate that the oxidation product of ascorbic acid is not reduced during the cathodic cycle such that the presence of ascorbic acid does not affect the detection of Fe(III). If instead of a current–potential diagram a current–time plot is recorded (see Fig. 5), then the maximum of the reduction current is a measure for the Fe(III) concentration during the reaction. A kinetic analysis of the concentration–time dependence following the initial concentration jump associated with dilution, results in $k_{obs}=(2.6\pm0.2)\times10^{-2}$ s^{-1} at 23.6 °C. The corresponding plot of $\ln(I_\infty - I_t)$ versus time was linear over three half-lives of the reaction. Stopped-flow experiments under similar conditions resulted in identical rate constants for the first decomposition reaction of the intermediate (see Fig. 2(b)). This indicates that oxidation of ascorbic acid by $Fe(C_2O_4)_3^{3-}$ occurs in the first reaction step observed during the decrease in absorbance of the intermediate complex, which also corresponds to the largest absorbance decrease observed for the two reaction steps.

In our earlier, less-sophisticated analysis of the redox process [10], the electron-transfer step was found to be independent of the ascorbate concentration, pH and ionic strength of the medium, which was interpreted in terms of the operation of only an inner-sphere redox process. These observations could not be reproduced when analysing the complete kinetic trace as done in this study. The observed rate constant exhibits a meaningful increase on increasing the ascorbate concentration

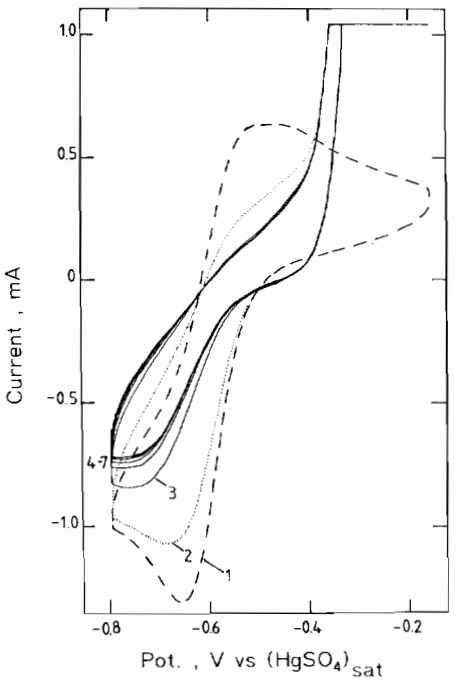

Fig. 4. Continuously recorded cyclovoltammograms during the decomposition of the intermediate produced in the reaction of $Fe(C_2O_4)_3^{3-}$ with L-ascorbic acid. Experimental conditions: $[AH_2]_{tot}=0.10$ M; $[oxalate]_{tot}=1.0\times10^{-2}$ M; $[Fe(C_2O_4)_3^{3-}]=2.0\times10^{-3}$ M; pH = 4.5 (acetate buffer); ionic strength = 1.0 M ($LiClO_4$); temperature = 23.6 °C, $dPot/dt = 200$ mV/s. Curve 1: CV of $Fe(C_2O_4)_3^{3-}$ solution prior to addition of L-ascorbic acid. Curves 2–7: CVs recorded immediately after addition of L-ascorbic acid.

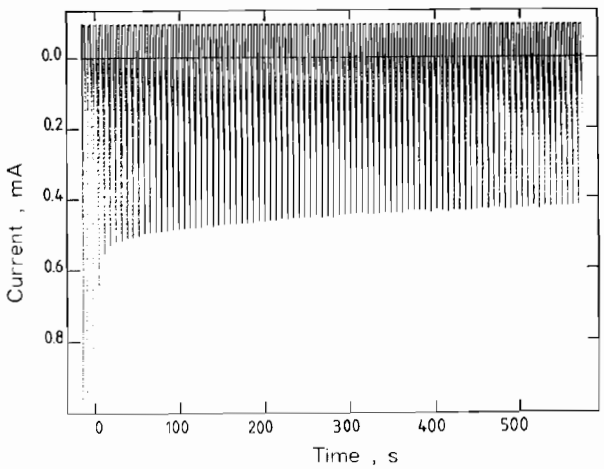

Fig. 5. Current–time plot for the CVs recorded in Fig. 4. Experimental conditions: see Fig. 4.

and pH of the reaction mixture, as well as a moderate decrease with increasing oxalate concentration. The kinetic data for both the decomposition steps, i.e. for the redox process (k_A) and the subsequent slow reaction (k_B), are summarized in Table 2, from which the mentioned trends in k_A can be clearly seen. These concentration dependences can be interpreted in terms of two parallel electron-transfer processes as indicated in eqn. (5), according to which $Fe(C_2O_4)_3^{3-}$ reacts with AH^- in an inner-sphere and outer-sphere way. The formation of the intermediate $Fe(C_2O_4)_2AH^{2-}$ species (see reaction (2)) can be considered as a pre-equilibrium step on the time scale of the redox process, for which $K_3 = K_1K_2$. The corresponding expression for the

$$\begin{array}{ccc} Fe(C_2O_4)_3^{3-} + AH^- & \overset{K_3}{\rightleftharpoons} & Fe(C_2O_4)_2AH^{2-} + C_2O_4^{2-} \\ \downarrow k_{os} & & \downarrow k_{is} \\ Fe(C_2O_4)_3^{4-} + {}^{\bullet}AH & & Fe(C_2O_4)_2^{2-} + {}^{\bullet}AH \end{array} \qquad (5)$$

$$^{\bullet}AH + Fe(III) \xrightarrow{fast} A + H^+ + Fe(II)$$

observed rate constant is given in eqn. (6), from which it follows that a plot of $k_A\{[C_2O_4^{2-}] + K_3[AH^-]\}/[AH^-]$ versus $[C_2O_4^{2-}]$ should be linear for all the data in Table 2. This is indeed the case as shown in Fig. 6, from which it follows that $k_{os} = 0.071 \pm 0.005$ M^{-1} s^{-1} and $k_{is} = 0.037 \pm 0.002$ s^{-1} (with $K_3 = 0.051$).

$$k_A = \frac{2(k_{os}[C_2O_4^{2-}][AH^-] + k_{is}K_3[AH^-])}{[C_2O_4^{2-}] + K_3[AH^-]} \qquad (6)$$

An increase in the oxalate concentration shifts the pre-equilibrium to the $Fe(C_2O_4)_3^{3-}$ species and favours the outer-sphere reaction path, whereas an increase in the ascorbate concentration will shift the pre-equilibrium to the $Fe(C_2O_4)_2AH^{2-}$ species in favour of the inner-sphere reaction path, although it will also increase the rate of the outer-sphere process. The increase in k_A with increasing pH is once again ascribed to the higher substitution and redox reactivity of AH^- as compared to AH_2 [1–5]. In addition, the inner-sphere pre-equilibrium (K_3) will depend on pH due to the protonation of AH^- and $C_2O_4^{2-}$ at lower pH. In the mechanism suggested in eqn. (5) we do not include a possible outer-sphere redox reaction between $Fe(C_2O_4)_2(H_2O)_2^-$ and AH^- (see reaction (2)), since this species will only be present at low concentrations ($K_1 = 1.41 \times 10^{-5}$ M [13]).

A direct comparison of the values of k_{os} and k_{is} is not possible due to the difference in reaction order. In terms of an outer-sphere electron-transfer reaction, k_{os} can be analysed in terms of a precursor formation constant (K_{os}) and an outer-sphere electron-transfer rate constant (k_{et}), since $k_{os} = K_{os}k_{et}$. A direct comparison of k_{et} and k_{is} will then be possible. K_{os} can be estimated on the basis of the Fuoss equation (7), where $\sigma (= r_1 + r_2)$ represents the distance of the ions and W_{ij} the electric work required to bring the ions together. The

$$K_{os} = \frac{4}{3}\pi N_A \sigma^3 \exp(-W_{ij}/RT) \qquad (7)$$

TABLE 2. Observed rate constants for the second and third reactions as a function of pH, ascorbic acid and oxalate concentration[a]

pH	$[H_2A]_{tot}$ (M)	$[oxalate]_{tot} \times 10^2$ (M)	$k_A{}^b \times 10^2$ (s^{-1})	$k_B{}^b \times 10^3$ (s^{-1})
4.0	0.10	1.0	1.48 ± 0.01	1.94 ± 0.05
4.25			2.32 ± 0.05	3.67 ± 0.14
4.5			3.00 ± 0.10	4.59 ± 0.20
5.0			4.89 ± 0.06	7.98 ± 0.09
4.5	0.15	1.0	4.10 ± 0.04	6.02 ± 0.06
		1.5	3.68 ± 0.09	5.73 ± 0.23
		2.0	3.33 ± 0.07	5.29 ± 0.12
		2.5	3.14 ± 0.11	5.08 ± 0.32
		3.0	3.02 ± 0.30	5.72 ± 0.58
4.5	0.30	1.5	5.60 ± 0.18	8.83 ± 0.20
		2.0	5.31 ± 0.16	8.51 ± 0.19
		2.5	4.85 ± 0.10	7.16 ± 0.09
		3.0	4.97 ± 0.22	6.78 ± 0.37
4.5	0.10	2.0	2.17 ± 0.08	3.76 ± 0.22
	0.15		3.33 ± 0.07	5.29 ± 0.12
	0.20		4.26 ± 0.06	6.52 ± 0.10
	0.25		4.98 ± 0.09	7.53 ± 0.13

[a]Experimental conditions: $[Fe(III)] = 2 \times 10^{-3}$ M; acetate buffer; ionic strength = 1.0 M; temperature = 25 °C. [b]Mean value of at least five kinetic runs.

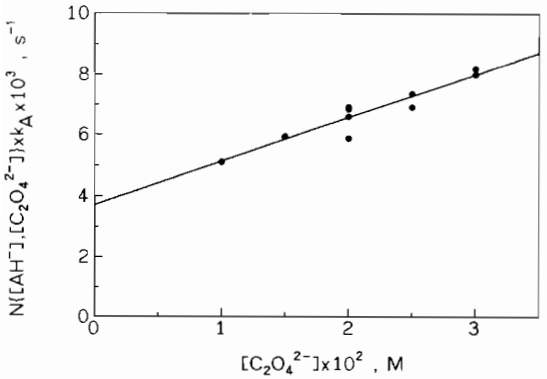

Fig. 6. Plot of k_A $\{[C_2O_4^{2-}]+K_3[AH^-]\}/[AH^-]$ vs. oxalate concentration for the data in Table 2 according to eqn. (6); $N\{[AH^-], [C_2O_4^{2-}]\}=\{[C_2O_4^{2-}]+K_3[AH^-]\}/[AH^-]$.

latter term can be calculated from eqn. (8), where Z_i and Z_j represent the charge on the ions, e_0 the

$$W_{ij}=Z_iZ_je_0^2N_A/4\pi\epsilon_0\epsilon\sigma(1+\chi\sigma) \quad (8)$$

elementary charge, ϵ_0 the dielectric constant of vacuum, ϵ the dielectric constant of the medium and χ the permeability of the medium as given by eqn. (9). For aqueous solutions at 25 °C, $\epsilon=78.4$ and $\chi=3.29\sqrt{\mu}$ nm^{-1} with the ionic strength μ in mol dm^{-3}.

$$\chi=(2e_0^2N_A\mu/\epsilon_0\epsilon k_BT)^{1/2} \quad (9)$$

With $r(AH^-)=0.33$ and $r(Fe(C_2O_4)_3^{3-})=0.39$ nm*, it follows that $W_{ij}=2.17$ kJ mol^{-1} and $K_{os}=0.40$ M^{-1}. The latter value is in close agreement with the value of 0.58 M^{-1} calculated for the $Fe(CN)_6^{3-}/AH^-$ system [1]. Combining this value with that of k_{os} results in $k_{et}=0.18$ s^{-1}. It follows that k_{et} is approximately five times larger than k_{is} under the present experimental conditions, i.e. electron transfer in the outer-sphere precursor species seems to be more effective than electron-transfer in the intermediate, inner-sphere species. This trend must be related to the change in redox potential of the Fe(III) species during substitution of oxalate by ascorbate. Further mechanistic differentiation will only be possible with the aid of activation parameters ($\Delta H^{\neq}$, $\Delta S^{\neq}$ and $\Delta V^{\neq}$) for these processes, but their determination is almost an impossible task due to the complexity of the kinetic behaviour of this system.

Kinetic data for the second step associated with the apparent decrease in concentration of the intermediate species, i.e. k_B, are included in Table 2. It should be noted that there is a large uncertainty involved in the estimation of k_B, and these data should not be over-interpreted. In general, k_B increases with increasing ascorbate concentration at a constant oxalate concentration, whereas k_B decreases slightly with increasing oxalate concentration at a constant ascorbate concentration. These trends can be interpreted in terms of a subsequent substitution reaction of the produced Fe(II) oxalato complex as shown in eqn. (10), since these reactions were performed in an excess of

$$Fe(C_2O_4)_3^{4-}+AH^- \rightleftharpoons Fe(C_2O_4)_2AH^{3-}+C_2O_4^{2-} \quad (10)$$

ascorbate. Whatever the detailed nature of the second decomposition step, it does not contribute significantly towards the observed electron-transfer process (k_A), but must be included in order to account for the observed kinetic traces. The intimate detail of the substitution reaction suggested in eqn. (11) may include rapid substitution of $Fe(C_2O_4)_2(H_2O)_2^{2-}$ by $C_2O_4^{2-}$, as well as ring-opening and ring-closure reactions of oxalate and ascorbate ligands.

Conclusions

The results of this investigation have clearly demonstrated the advantage of using sophisticated data acquisition and analysis systems in the study of complex kinetic processes. In addition, they have revealed direct evidence for the occurrence of two parallel electron-transfer processes which have been assigned to inner-sphere and outer-sphere redox reactions. A similar situation was suggested to account for the observed kinetic data for the oxidation of L-ascorbic acid by aquated Fe(III), for which the more labile $Fe(H_2O)_5OH^{2+}$ species prefers the inner-sphere, and the less labile $Fe(H_2O)_6^{3+}$ species the outer-sphere reaction routes [6]. In the present system, $Fe(C_2O_4)_3^{3-}$ reacts with AH^- via both outer-sphere and inner-sphere reaction paths involving the formation of the $Fe(C_2O_4)_2AH^{2-}$ intermediate in the latter case. In the case of non-labile complexes such as $Fe(CN)_6^{3-}$, $Fe(phen)_3^{3+}$ and $Fe(sar)^{3+}$, only an outer-sphere electron-transfer process can occur.

Finally, the value of k_{os} for the outer-sphere electron-transfer reaction between $Fe(C_2O_4)_3^{3-}$ and HA^- found in this study enables us to estimate the self-exchange rate constant for $Fe(C_2O_4)_3^{3-/4-}$ and to compare the latter value with data available for related systems. According to the Marcus cross relationship in eqn. (11), the self-exchange rate constant for $Fe(C_2O_4)_3^{3-/4-}$ (k_{11}) was estimated from $k_{22}=1.60\times10^5$ M^{-1} s^{-1}, the self-exchange rate constant for $^{\cdot}AH/AH^-$ [1], and $K_{12}=1.47\times10^{-12}$**, and has the value 2.1×10^4 M^{-1} s^{-1}. This value can now be compared with those

*The radius of $Fe(C_2O_4)_3^{3-}$ was estimated from the density of $K_3Fe(C_2O_4)_3$, viz. 2.133 g cm^{-3}.

**K_{12} is the equilibrium constant of the unsymmetrical redox process and was estimated from $E^0_{11}=0.01$ V [14] and $E^0_{22}=0.71$ V [15–17].

TABLE 3. Summary of available self-exchange electron transfer rate constants for Fe complexes

System[a]	k_{11} (M^{-1} s^{-1})	Reference
$Fe(CN)_6^{3-/4-}$	1.9×10^4	18
$Fe(H_2O)_6^{3+/2+}$	*c.* 8	19
$Fe(C_2O_4)_3^{3-/4-}$	2.1×10^4	this work
$Fe(sar)^{3+/2+}$	6.0×10^3	20
$Fe(phen)_3^{3+/2+}$	1.3×10^7	21
$Fe(imid)_2(Ph_4por)^{3+/2+}$	8.1×10^7	22

[a]sar = 3, 6, 10, 13, 16, 19-hexaazabicyclo[6.6.6]eicosan; phen = 1,10-phenanthroline; imid = imidazole; Ph_4por = tetraphenylporphyrin.

$$k_{os}=(k_{11}k_{22}K_{12}f)^{1/2}\ (f=1) \tag{11}$$

for related systems, summarized in Table 3. It follows that k_{11} for $Fe(C_2O_4)_3^{3-/4-}$ agrees exactly with that for $Fe(CN)_6^{3-/4-}$ and is close to that for $Fe(sar)^{3+/2+}$, considerably larger than for $Fe(H_2O)_6^{3+/2+}$, and considerably smaller than for $Fe(phen)_3^{3+/2+}$ and $Fe(imid)_2(Ph_4por)$. The large values of k_{11} found for most of the complexes can be ascribed to a low internal reorganization energy (ΔG^*) required for the self-exchange process. In addition, the π-conjugated ligands present in some systems (phenanthroline and imidazole) can further assist the electron-transfer step and account for the very high values of k_{11}. The extreme low value of k_{11} for $Fe(H_2O)_6^{3+/2+}$ may be related to the large outer reorganization energy (solvational changes) associated with this process.

Acknowledgements

The authors gratefully acknowledge financial support from the Deutsche Forschungsgemeinschaft, Fonds der Chemischen Industrie, and DAAD for a fellowship to P.M.

References

1 B. Bänsch, P. Martinez, D. Uribe and R. van Eldik, *Z. Phys. Chem., 170* (1991) 59.
2 E. Pelizetti, E. Mentasti and E. Pramauro, *Inorg. Chem., 15* (1976) 2898.
3 M. Kimura and M. Yamamoto, *J. Chem. Soc., Dalton Trans.,* (1982) 423.
4 K. Tsukahara and Y. Yamamoto, *Bull. Chem. Soc. Jpn., 54* (1981) 2642.
5 R. A. Rickman, R. L. Sorensen, K. O. Watkins and G. Davies, *Inorg. Chem., 16* (1977) 1570.
6 B. Bänsch, P. Martinez, D. Uribe, J. Zuluaga and R. van Eldik, *Inorg. Chem., 30* (1991) 4555.
7 S. Gangopadhyay, S. Saha, M. Ali and P. Banerjee, *Int. J. Chem. Kinet., 23* (1991) 105.
8 M. M. Taqui Khan and R. S. Shukla, *Inorg. Chim. Acta, 149* (1988) 89.
9 Y. Xu and R. B. Jordan, *Inorg. Chem., 29* (1990) 4180, and refs. therein.
10 P. Martinez, J. Zuluaga, D. Uribe and R. van Eldik, *Inorg. Chim. Acta, 136* (1987) 11.
11 *OLIS KINET*, Olis Inc., Jefferson, GA 30549, USA.
12 K. Schneider and R. van Eldik, *Organometallics, 9* (1990) 92.
13 A. E. Martell and R. M. Smith, *Critical Stability Constants,* Vol. 3, Plenum, New York, 1977, p. 94.
14 J. C. Myland, K. B. Oldham and C. G. Zoski, *J. Electroanal. Chem., 193* (1985) 3.
15 D. H. Macartney and N. Sutin, *Inorg. Chim. Acta, 74* (1983) 221.
16 N. H. Williams and J. K. Yandell, *Aust. J. Chem., 35* (1982) 1133.
17 S. Steenken and P. Neta, *J. Phys. Chem., 83* (1979) 1134.
18 A. J. Miralles, R. E. Armstrong and A. Haim, *J. Am. Chem. Soc., 99* (1977) 1416; A. Haim and N. Sutin, *Inorg. Chem., 15* (1976) 476.
19 W. H. Jolley, D. R. Stranks and T. W. Swaddle, *Inorg. Chem., 29* (1990) 1948.
20 P. Bernhard and A. M. Sargeson, *Inorg. Chem., 26* (1987) 4122.
21 H. Doine and T. W. Swaddle, *Can. J. Chem., 66* (1988) 2763.
22 A. Shirazi, M. Barbush, S. Ghosh and D. W. Dixon, *Inorg. Chem., 24* (1985) 2495.